A benzene-core trinuclear Gd^{III} complex: towards the optimization of relaxivity for MRI contrast agent applications at high magnetic field†

João Bruno Livramento,[a] Lothar Helm,[a] Angélique Sour,[a] Conlin O'Neil,[b] André E. Merbach[a] and Éva Tóth*[a,c]

Received 9th November 2007, Accepted 20th November 2007
First published as an Advance Article on the web 20th December 2007
DOI: 10.1039/b717390c

A novel ligand, $H_{12}L$, based on a trimethylbenzene core bearing three methylenediethylenetriamine-*N*,*N*,*N*″,*N*″-tetraacetate moieties ($-CH_2DTTA^{4-}$) for Gd^{3+} chelation has been synthesized, and its trinuclear Gd^{3+} complex $[Gd_3L(H_2O)_6]^{3-}$ investigated with respect to MRI contrast agent applications. A multiple-field, variable-temperature ^{17}O NMR and proton relaxivity study on $[Gd_3L(H_2O)_6]^{3-}$ yielded the parameters characterizing water exchange and rotational dynamics. On the basis of the ^{17}O chemical shifts, bishydration of Gd^{3+} could be evidenced. The water exchange rate, $k_{ex}^{298} = 9.0 \pm 3.0\ s^{-1}$ is around twice as high as k_{ex}^{298} of the commercial $[Gd(DTPA)(H_2O)]^{2-}$ and comparable to those on analogous Gd^{3+}-DTTA chelates. Despite the relatively small size of the complex, the rotational dynamics had to be described with the Lipari–Szabo approach, by separating global and local motions. The difference between the local and global rotational correlation times, $\tau_{lO}^{298} = 170 \pm 10$ ps and $\tau_{gO}^{298} = 540 \pm 100$ ps respectively, shows that $[Gd_3L(H_2O)_6]^{3-}$ is not fully rigid; its flexibility originates from the CH_2 linker between the benzene core and the poly(amino carboxylate) moiety. As a consequence of the two inner-sphere water molecules per Gd^{3+}, their close to optimal exchange rate and the appropriate size and limited flexibility of the molecule, $[Gd_3L(H_2O)_6]^{3-}$ has remarkable proton relaxivities when compared with commercial contrast agents, particularly at high magnetic fields (r_1 = 21.6, 17.0 and 10.7 $mM^{-1}s^{-1}$ at 60, 200 and 400 MHz respectively, at 25 °C; r_1 is the paramagnetic enhancement of the longitudinal water proton relaxation rate, referred to 1 mM concentration of Gd^{3+}).

Introduction

In the last two decades, magnetic resonance imaging (MRI) has become one of the most prominent techniques in clinical diagnostics and biomedical research. In MRI, the amount of available signal is inextricably associated with the static magnetic field strength. Higher field strength offers considerable improvement in the signal-to-noise ratio (proportional to $B_0^{7/4}$ at mid-fields, with a more linear dependence at high fields), which translates to an increased spatial and temporal resolution. In addition, T_1 relaxation times of grey and white matter also increase with field strength, thus at high field the uptake of a contrast agent will result in a more significant shortening of T_1. Until recently, common clinical scanners operated at ≤1.5 T. Due to recent improvements in magnet design, 3 T scanners have become widely available in the clinics, and for experimental animal studies much higher fields (≥9.4 T; 400 MHz) have entered the everyday practice.[1]

Gd^{3+} complexes are widely used to increase image contrast in MRI.[2,3] Their efficiency is expressed by their proton relaxivity, r_1, which is the paramagnetic enhancement of the longitudinal water proton relaxation rate, in reference to a 1 mM concentration of Gd^{3+}. Proton relaxivity is directly related to the microscopic parameters of the chelate, such as water exchange, rotational dynamics or electronic relaxation. Much effort has been devoted to the optimization of these factors on Gd^{3+} complexes with the objective of increasing relaxivity. In particular, slowing down the rotation by using macromolecules resulted in a remarkable relaxivity improvement at intermediate frequencies (20–60 MHz) as compared to commercial agents.[2–4] For macromolecular agents, however, above 60 MHz r_1 drops strongly with increasing magnetic field and, at high frequencies (above 100 MHz), they are hardly superior to small chelates. The optimization of the relaxivity at high magnetic field requires the fine-tuning of the microscopic parameters of the Gd^{3+} complex to optimal values which are different from those at intermediate fields. Namely, as the Solomon–Bloembergen–Morgan theory predicts, at proton Larmor frequencies above 200 MHz r_1 increases with the inverse rotational correlation time $1/\tau_R$, in contrast to lower frequencies where it is proportional to τ_R (Fig. 1). Thus at high frequencies, rigid molecules of intermediate size are favoured over large ones, with an optimal τ_R of ~400 ps at 400 MHz (the exact value of the optimal rotational correlation time will also be dependent on the other influencing parameters). One peculiarity of high field optimization is that the optimal rotational correlation time is very sensitive to the magnetic field but remains, nevertheless, in the range of 400–1000 ps. The optimal value of the water exchange

[a]*Institut des Sciences et Ingénierie Chimiques, École Polytechnique Fédérale de Lausanne, ISIC, BCH, CH-1015, Lausanne, Switzerland; Fax: +41 (0)21 693 9875; Tel: +41 (0)21 693 98 71*
[b]*Laboratoire de médecine régénérative et de pharmacobiologie, École Polytechnique Fédérale de Lausanne, EPFL-AAB, CH-1015, Lausanne, Switzerland*
[c]*Centre de Biophysique Moléculaire, CNRS, rue Charles Sadron, 45071, Orléans, France. E-mail: eva.jakabtoth@cnrs-orleans.fr; Fax: +33 (0)2 3863 1517; Tel: +33 (0)2 3825 7625*

† Electronic supplementary information (ESI) available: Equations used in the analysis of ^{17}O NMR and NMRD data; experimental data of proton relaxivities, ^{17}O relaxation rates and chemical shifts, details of HPLC separation. See DOI: 10.1039/b717390c

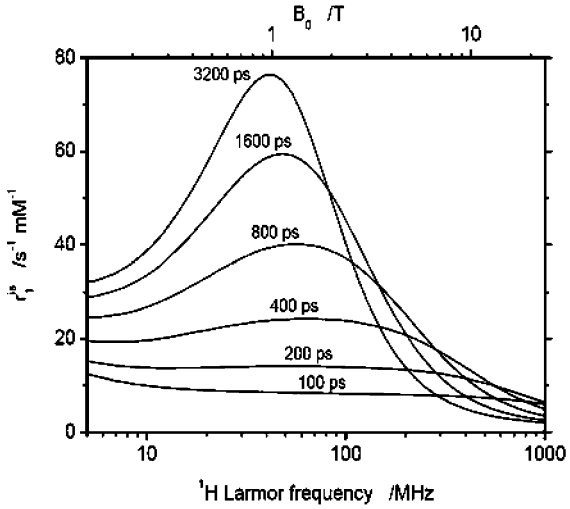

Fig. 1 Inner sphere proton relaxivities calculated using the Solomon–Bloembergen–Morgan theory for various values of the rotational correlation time, τ_R, as a function of the magnetic field (upper *x*-axis) or the proton Larmor frequency (lower *x*-axis). $q = 2$, $k_{ex} = 9 \times 10^6\ s^{-1}$, $\tau_v = 38$ ps, $\Delta^2 = 0.1 \times 10^{20}\ s^{-2}$.

rate will also be different (and considerably higher) from that for current clinical fields.[5] The development of contrast agents specifically designed for high field applications is an emerging domain, and apart from some preliminary studies,[6–8] no dedicated agents have been reported. We recently published a self-assembled, metallostar-structured system, $\{Fe[Gd_2bpy(DTTA)_2(H_2O)_4]_3\}^{4-}$, with a remarkable relaxivity at high magnetic fields (r_1 = 15.8 $mM^{-1}\ s^{-1}$ at 4.7 T and 37 °C; Scheme 1).

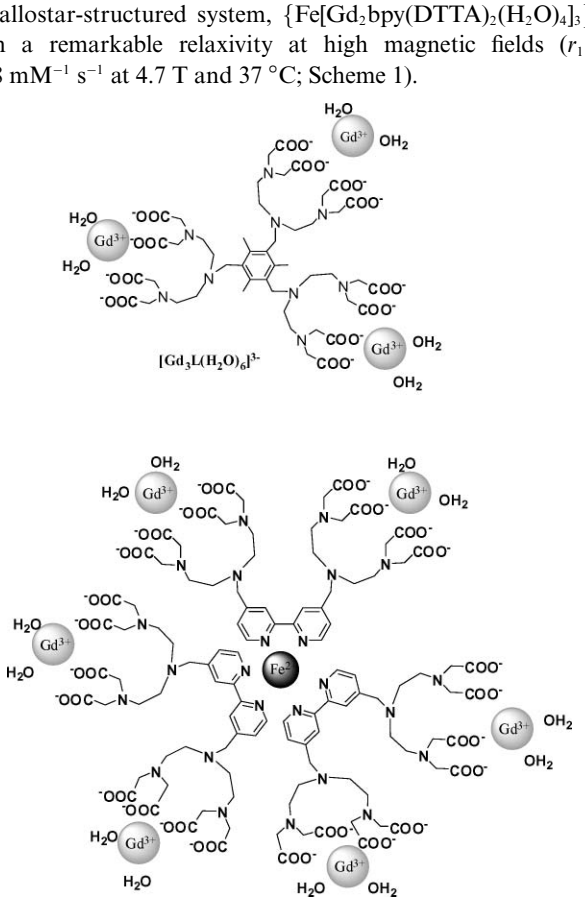

Scheme 1 Structure of potential high field MRI contrast agents.

MR imaging experiments at 4.7 T confirmed the good contrast agent efficiency of the metallostar under *in vivo* conditions.[9] Nevertheless, one drawback of this system is the limited stability of the Fe^{2+}-tris(bipyridine) core, which might lead to slow decomposition of the metallostar in biological conditions,[8] and hence raise free iron toxicity concerns. In order to overcome this problem, we have designed a novel chelate, $H_{12}L$, involving covalent linking of three DTTA units to a central trimethylbenzene core ($-CH_2DTTA^{4-}$) = methylenediethylenetriamine-*N*,*N*,*N*″,*N*″-tetraacetate). $H_{12}L$ affords a trinuclear Gd^{3+} complex (Scheme 1) of medium size with a rotational correlation time expected to be in the appropriate range to attain maximum relaxivities at 4.7–9.4 T. The $DTTA^{4-}$ chelator has been previously proved to possess several positive features with regard to MRI contrast agent applications. It guarantees a relatively fast water exchange on the Gd^{3+} complex, as evidenced for analogue chelates.[8,10] The complex has two inner sphere water molecules to double the inner sphere relaxivity contribution. The animal imaging results obtained with the metallostar[9] showed that the efficiency of the chelate is not reduced *in vivo*, which proves that the two inner sphere water molecules in $GdDTTA^-$ are not replaced by endogenous anions or other potential donors from proteins *etc.* in the biological medium. This is an important feature in favour of the DTTA-chelates in comparison with the macrocyclic bishydrated LnDO3A complexes, known for their ability to form ternary complexes with various endogenous carboxylate donors.[11]

For *in vivo* applications, the Gd^{3+} chelate has to be sufficiently stable so that no release of free Gd^{3+} occurs before total excretion of the contrast agent from the body. Thermodynamic stability was assessed for several $GdDTTA^-$-type complexes and showed a limited decrease compared to $[Gd(DTPA)(H_2O)]^{2-}$. The stability constants determined for the Gd^{3+} complexes formed with DTTA-chelators attached to a benzene or a bipyridine core were all in the range of log K_{GdL} = 17–19, with corresponding pGd values of ~15–16 ($[L]_{total} = 10\ \mu M$; $[Gd]_{total} = 1\ \mu M$; pH = 7.4).[8,10] Evidently, these stabilities would not be acceptable for human applications, nevertheless, they can be sufficient for animal studies.[12] In fact, high field imaging is essentially intended for animal experiments.

We have previously reported the synthesis and physico-chemical characterization of dinuclear, bishydrated Gd^{3+} complexes $[Gd_2(m\text{-}X(DTTA)_2)(H_2O)_4]^{2-}$ and $[Gd_2(p\text{-}X(DTTA)_2)(H_2O)_4]^{2-}$, based on a xylene core substituted in *para* and *meta* positions by the same DTTA chelators as in ligand L (X = xylene).[10] These complexes have elevated proton relaxivities at high field. On introducing a third DTTA unit and replacing the benzene core with 1,3,5-trimethylbenzene, we expected a further rigidification of the molecule, a slightly longer rotational correlation time and a concomitant increase in the high field relaxivities.

Here we report the synthesis of ligand $H_{12}L$ and the physico-chemical characterization of its trinuclear Gd^{3+} complex, $[Gd_3L(H_2O)_6]^{3-}$. We have performed a combined ^{17}O NMR and ^1H NMRD (nuclear magnetic relaxation dispersion) study which allowed us to assess all significant parameters influencing proton relaxivity. The promising *in vitro* relaxivities obtained at high magnetic fields prompted us to pursue the assessment of this trinuclear Gd^{3+} chelate in *in vivo* animal imaging experiments at 9.4 T. These results, to be published elsewhere,[13] confirmed the considerably higher efficacy of the complex with respect to commercial contrast agents in high field applications.

Results and discussion

Synthesis

The synthesis of ligand $H_{12}L$ is presented in Scheme 2. The synthetic route is composed of two major steps: synthesis of the tetraester amine compound **4** and its conjugation onto the alkyl halide 1,3,5-tris(bromomethyl)-2,4,6-trimethylbenzene, which is subsequently hydrolyzed to give the desired ligand **6**. Compound **4** was prepared in a succession of protection/deprotection steps. Two consecutive protections are done, first on the terminal primary amines of the diethylenetriamine (to form compound **1**), and second on the central secondary amine to yield compound **2**. Deprotections of both amines are done selectively. The terminal amines are first deprotected and then alkylated with *t*-butylbromoacetate to give compound **3**. The central amine is then deprotected with Pd over charcoal to yield the building block **4**. Reaction of 1,3,5-tris(bromomethyl)-2,4,6-trimethylbenzene with compound **4** in the presence of K_2CO_3 gave the ester **5**, which was hydrolyzed to the product **6**. This desired trisubstituted ligand $H_{12}L$ was obtained as a mixture with the corresponding disubstituted molecule where the third arm previously bearing a bromine has been converted into an alcohol.

The separation of these two similar compounds proved to be hard. It was attempted on a cationic exchange resin, which is a conventional separation method for poly(amino carboxylates). However, the separation was revealed to be unsuccessful even when repeated. Therefore we have performed an HPLC separation by using ESI-MS and UV-Vis spectroscopy as combined detection methods. The purity of the desired product was further confirmed by ^{1}H NMR spectroscopy.

Molecular modelling

The spatial demand of the tris-DTTA substitution on the trimethylbenzene core was assessed by molecular modelling studies. As Fig. 2 shows, the molecule bearing three DTTA-units in 1,3,5-positions of the central benzene is not sterically overcrowded. The exact Gd-Gd distances are determined at any given time by the conformation of the methylene bridges linking the DTTA unit on the central nitrogen to the benzene ring.

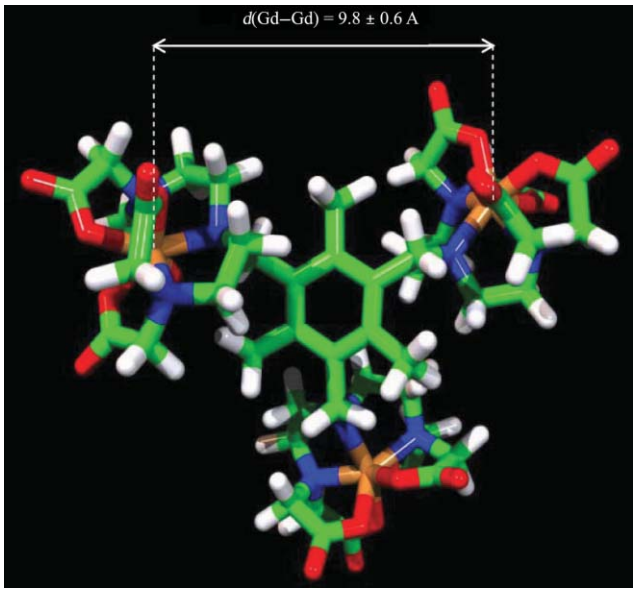

Fig. 2 Molecular modelling representation of $[Gd_3L(H_2O)_6]^{3-}$.

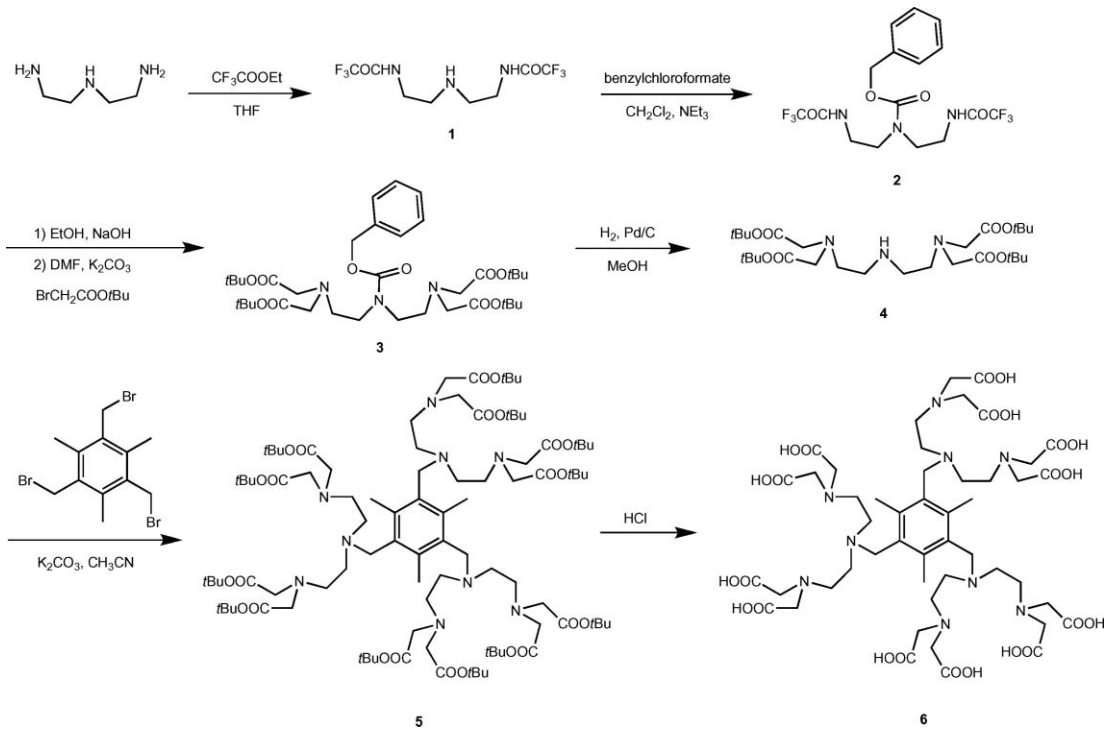

Scheme 2 Synthesis of $H_{12}L$.

However a rough estimation of the average distance could be made: d(Gd–Gd) = 9.8 ± 0.6 Å. This distance is long enough to preclude important dipolar interactions between Gd^{3+} ions that could accelerate electronic relaxation and cut back relaxivity at high magnetic fields.[14]

^{17}O NMR and ^{1}H NMRD measurements

The parameters characterizing water exchange and rotation of $[Gd_3L(H_2O)_6]^{3-}$ were obtained in a variable-temperature, multiple-field ^{17}O NMR and ^{1}H NMRD study (Fig. 3). The ^{17}O longitudinal and transverse relaxation rates and chemical shifts were measured in an aqueous solution of $[Gd_3L(H_2O)_6]^{3-}$ at 4.7 and 9.4 T. Relaxivity measurements were performed between 0.01–400 MHz proton Larmor frequency at 5, 25 and 37 °C. The reduced ^{17}O transverse relaxation rates, $1/T_{2r}$, attain a maximum at ~283 K. Above this value, they decrease with increasing temperature indicating a fast exchange region. Here $1/T_{2r}$ is given by the transverse relaxation rate of the bound water oxygen, $1/T_{2m}$, which is influenced by the water exchange rate, k_{ex}, the scalar coupling constant, $A/$, and the longitudinal electronic relaxation rate, $1/T_{1e}$.

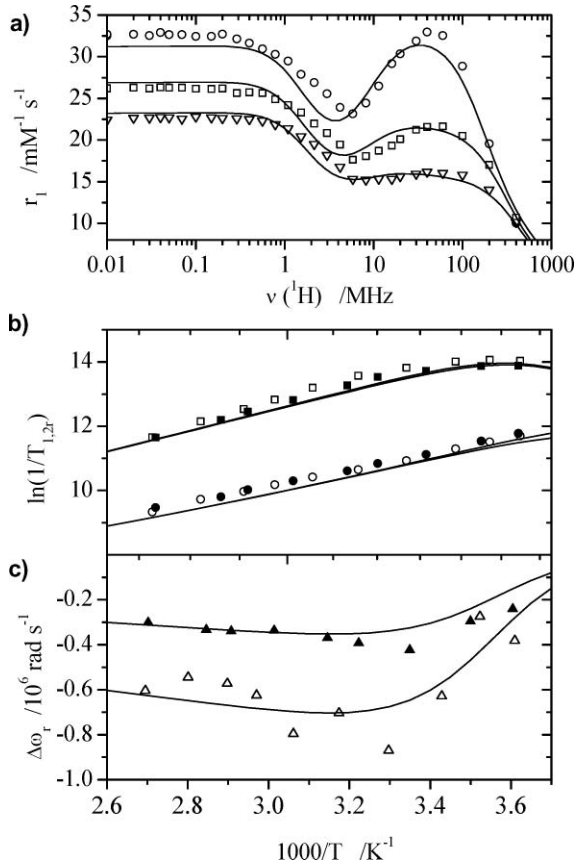

Fig. 3 (a) ^{1}H nuclear magnetic relaxation dispersion profiles, recorded at 5 (○), 25 (□) and 37 °C (▽); temperature dependence of (b) reduced transverse $1/T_{2r}$ [9.4 (□) and 4.7 T (■)] and longitudinal $1/T_{1r}$ ^{17}O relaxation rates [9.4 T (○) and 4.7 T (●)]; and (c) reduced chemical shifts $\Delta\omega_r$ [9.4 (Δ) and 4.7 T (▲)]. The lines represent the least-squares simultaneous fitting of all data points.

The transverse ^{17}O relaxation proceeds *via* a scalar mechanism and holds no rotational information. This latter is contained in the longitudinal ^{17}O relaxation, which is governed by dipole–dipole (influenced by the Gd^{3+}–water oxygen distance, r_{GdO}) and quadrupolar mechanisms (influenced by the quadrupolar coupling constant, $\chi(1 + \eta^2/3)^{1/2}$).

The ^{17}O relaxation rates and chemical shifts and the proton relaxivity data were analyzed simultaneously on the basis of the Solomon–Bloembergen–Morgan theory.[16] The rotational dynamics has been described by using the Lipari–Szabo approach which allows the separation of the local motion of the Gd^{3+} chelating subunits, characterized by a local rotational correlation time, τ_l, from the motion of the overall molecule, described by an overall rotational correlation time, τ_g.[17,18] Despite the relatively small size of $[Gd_3L(H_2O)_6]^{3-}$, we could not achieve a satisfactory fit of the NMRD curves by using a single rotational correlation time and the Lipari–Szabo treatment was necessary.

In the fitting procedure several parameters were fixed to common values. The distance between the Gd^{3+} electron spin and the coordinated water ^{17}O nucleus, r_{GdO}, was considered to be 2.50 Å, based on available crystal structures[19] and ESEEM data.[20] The Gd^{3+}–H distance, r_{GdH}, was set to 3.10 Å, and the distance of closest approach of an outer sphere water proton to Gd^{3+}, a_{GdH}, to 3.5 Å. The quadrupolar coupling constant, $\chi(1+\eta^2/3)^{1/2}$) was 7.58 MHz, the value for pure water.

The scalar coupling constant calculated for $[Gd_3L(H_2O)_6]^{3-}$ is $A/ = -(3.4 \pm 0.7) \times 10^6$ rad s^{-1}. For the electron spin relaxation, the following parameters have been obtained: $E_v = 0.5$ kJ mol^{-1}; $\tau_v^{298} = 38 \pm 5$ ps, $\Delta^2 = (0.1 \pm 0.02) \times 10^{20}$ s^{-2}. In addition to the static zero field splitting contribution, a spin rotation term has been also included, characterized by the parameter $\delta g_L^2 = 0.1$. The diffusion constant, D_{GdH}^{298}, and its activation energy, E_{GdH}, were 20×10^{-10} m^2 s and 23 kJ mol^{-1} respectively.

The motions of the Gd-coordinated water oxygen and the Gd-coordinated water hydrogen vectors are reflected in the longitudinal ^{17}O and ^{1}H relaxation. The ratio between the local rotational correlation time of the Gd–H_{water} and Gd–O_{water} vectors, τ_{gH}/τ_{gO}, was fixed to 0.65, a usual value for this kind of complex.[21] All equations used in the analysis are given in the ESI† and the fitted curves are shown in Fig. 3. Tables 1 and 2 summarize the parameters characterizing water exchange and rotation respectively.

Water exchange

$DTTA^{4-}$ is a heptacoordinate ligand for Gd^{3+}, leaving two coordination sites to be occupied by water. Crystallographic data published on the analogous chelate $[(CNH_2)_3]_3$-[Gd(TTAHA)]·9H_2O proved the coordination of seven donor atoms of the poly(amino carboxylate) ($TTAHA^{6-}$ = *N*-tris(2-aminoethyl)amine-*N*′,*N*′,*N*″,*N*″,*N*‴,*N*‴-hexaacetate).[22] In this structure two binding sites were occupied by neighboring carboxylates which are then replaced by water molecules in aqueous solution. The bishydration of the lanthanide ion in $[Gd_3L(H_2O)_6]^{3-}$ has been confirmed by the experimental ^{17}O chemical shifts. UV-Vis measurements were previously performed on the dinuclear Eu^{3+} analogues *m*-X[Eu(DTTA)$(H_2O)_2]_2^{2-}$ and *p*-X[Eu(DTTA)$(H_2O)_2]_2^{2-}$ in the $^7F_0$–$^5D_0$ region which proved the absence of hydration equilibrium on DTTA-chelates.[10]

The water exchange parameters obtained in the fit are summarized in Table 1. As expected, the exchange rates of the various complexes carrying a DTTA unit are similar, with the

Table 1 Water exchange rates, k_{ex}^{298}, activation enthalpies, $\Delta H^{\ddagger}$, and activation entropies, $\Delta S^{\ddagger}$, of selected Gd^{3+} complexes

Complex	$k_{ex}^{298}/10^6\ s^{-1}$	$\Delta H^{\ddagger}$/kJ mol^{-1}	$\Delta S^{\ddagger}$/J mol^{-1} K^{-1}	Ref.
$[Gd_3L(H_2O)_6]^{3-}$	9 ± 3	40 ± 3	+31 ± 5	This work
$\{Fe[Gd_2bpy(DTTA)_2(H_2O)_4]_3\}^{4-}$	7.4	41.3	+25	8
$[Gd_2(m\text{-}X(DTTA)_2)(H_2O)_4]^{2-}$	8.9	39.2	+24	10
$[Gd_2(p\text{-}X(DTTA)_2)(H_2O)_4]^{2}$	9.0	45.4	+41	10
$[Gd(DTPA)(H_2O)]^{2-}$	3.3	51.6	+53	15

exception of $\{Fe[Gd(tpy\text{-}DTTA)(H_2O)_2]_2\}$ which has a lower k_{ex}, related to the neutrality of the complex. On the other hand, k_{ex} on $[Gd(DTPA)(H_2O)]^{2-}$ is almost half of that displayed by the DTTA-based complexes. The faster exchange on the DTTA-chelates can be rationalized in terms of their flexible inner sphere structure, induced by the presence of the two inner sphere water molecules. With respect to $[Gd(DTPA)(H_2O)]^{2-}$, this faster exchange could be beneficial in attaining higher relaxivities at any frequency, once the rotational dynamics are optimized. The values of activation entropy and enthalpy obtained for $[Gd_3L(H_2O)_6]^{3-}$ are in agreement with a dissociatively activated water exchange mechanism expected for a nine-coordinate complex.

Rotational dynamics

The rotational parameters calculated for $[Gd_3L(H_2O)_6]^{3-}$ are presented and compared to those of different size Gd^{3+} complexes in Table 2. The global rotational correlation time, τ_{gO}^{298}, is much lower than that for the metallostar and reflects the difference in their molecular weight. On the other hand, the local rotational correlation time, τ_{lO}^{298}, and the S^2 parameter characterizing the spatial restriction of the local with regard to the global motion are very similar for the two systems. This similarity can be expected, since in both cases the only relevant source of flexibility is the CH_2 moiety connecting the DTTA unit to the aromatic core. In accordance with this, no internal flexibility was observed for $\{Fe[Gd(tpy\text{-}DTTA)(H_2O)_2]_2\}$ in which the poly(amino carboxylate) is directly linked to the terpyridine unit.[24]

Although the CH_2 linker brings a certain flexibility to the molecule, its presence is necessary for stability reasons: the direct attachment of the amine of the DTTA chelator to a benzene ring is known to reduce the basicity of the nitrogen which then translates to a reduced stability of the Gd^{3+} complex.[24] In order to limit flexibility as much as possible, a 2,4,6-trimethyl derivative of benzene was used as the central core.

Proton relaxivity

$[Gd_3L(H_2O)_6]^{3-}$ displays considerably high relaxivities, although at medium field they are still limited by fast rotation as the temperature dependence of the relaxivity hump evidences (r_1 decreases with increasing temperature). At 20 MHz, the trinuclear complex has a relaxivity about four times higher than the commercial $[Gd(DOTA)(H_2O)]^{-}$ or $[Gd(DTPA)(H_2O)]^{2-}$ and it is close to the relaxivities of macromolecular, dendrimeric complexes such as Gadomer 17 (Table 2). Several factors account for the high r_1 value. $[Gd_3L(H_2O)_6]^{3-}$ is a rigid structure possessing three Gd^{3+} centers tightly bound around the benzene core. Each of these metal ions carries two inner sphere water molecules. Furthermore, the six inner sphere water molecules exchange with the bulk with a rate close to the optimal value.

Table 2 Rotational correlation times, τ_{RO}^{298}, proton relaxivities, r_1, and densities of relaxivity for selected Gd^{3+} complexes (20 MHz; 37 °C)

Complex	τ_{RO}^{298}/ps	r_1/mM^{-1} s^{-1}	Density of relaxivity/s^{-1} g^{-1} L	Ref.
$[Gd_3L(H_2O)_6]^{3-}$	$\tau_{gO}^{298} = 540 \pm 100$ $\tau_{lO}^{298} = 173 \pm 10^a$ $S^2 = 0.5 \pm 0.1$	15.7	29.0	This work
Small MW complexes				
$[Gd(DTPA)(H_2O)]^{2-}$	58	4.0	7.1	15
$[Gd(DOTA)(H_2O)]^{-}$	77	3.8	6.7	15
Dinuclear complexes				
$[Gd_2bpy(DTTA)_2(H_2O)_4]^{2-}$	240	12.4	20.2	8
$[Gd_2(m\text{-}X(DTTA)_2)(H_2O)_4]^{2-}$	278	5.8	14.3	10
$[Gd_2(p\text{-}X(DTTA)_2)(H_2O)_4]^{2}$	289	4.9	15.8	10
Heterometallic complexes				
$\{Fe[Gd(tpy\text{-}DTTA)(H_2O)_2]_2\}$	410	15.7	20.0	24
$\{Fe[Gd_2bpy(DTTA)_2(H_2O)_4]_3\}^{4-}$	$\tau_{gO}^{298} = 930$ $\tau_{lO}^{298} = 190$ $S^2 = 0.6$	20.1	32.2	8
Dendrimers				
Gadomer 17	$\tau_{gO}^{298} = 3050$ $\tau_{lO}^{298} = 760$ $S^2 = 0.5$	17.5	19.3	23

[a] $E_g = 23 \pm 3$ kJ mol^{-1}; $E_l = 22 \pm 8$ kJ mol^{-1}.

Table 3 High field relaxivities of selected Gd^{3+} complexes

r_1/mM^{-1} s^{-1}	200 MHz		400 MHz	
	25 °C	37 °C	25 °C	37 °C
$[Gd_3L(H_2O)_6]^{3-}$	17.0	14.1	10.7	10.2
$\{Fe[Gd_2bpy(DTTA)_2(H_2O)_4]_3\}^{4-}$ [a]	16.4	15.9	9.32	8.53
$[Gd_2(m\text{-}X(DTTA)_2)(H_2O)_4]^{2-}$ [b]	13.4	10.2	9.18	8.12
$[Gd_2(p\text{-}X(DTTA)_2)(H_2O)_4]^{2-}$ [b]	14.4	11.9	10.7	9.59
$[Gd(DOTA)(H_2O)]^{-}$ [c]	4.02	3.04	3.86	2.95
$[Gd(DTPA)(H_2O)]^{2-}$ [c]	4.22	3.20	4.06	3.13

[a] Ref. 8. [b] Ref. 10. [c] Ref. 9.

An important characteristic of the trinuclear complex is its exceptionally broad relaxivity hump centered around 30–60 MHz. In fact, the relaxivity is almost constant between 20 MHz (15.7 mM^{-1} s^{-1}, 37 °C) and 200 MHz (14.1 mM^{-1} s^{-1}, 37 °C). As expected, the high field relaxivities are considerably higher than those of $[Gd(DOTA)(H_2O)]^{-}$ and $[Gd(DTPA)(H_2O)]^{2-}$ (Table 3). However, they do not attain the maximum values which can be theoretically calculated on the basis of the Solomon–Bloembergen–Morgan theory by using the water exchange and electronic parameters as determined for $[Gd_3L(H_2O)_6]^{3-}$, and assuming optimal rotational dynamics, as shown in Fig. 1. The theoretically attainable relaxivities would be ~25 and 18 mM^{-1} s^{-1} at 200 and 400 MHz respectively (considering ~2 mM^{-1} s^{-1} for the outer sphere contribution). Instead of these values, for $[Gd_3L(H_2O)_6]^{3-}$ we measure 17.0 and 10.2 mM^{-1} s^{-1} at 200 and 400 MHz respectively. This difference clearly shows the importance of the rotational motion and in particular of the internal flexibility, responsible for cutting back the relaxivity.

It is interesting to note that at 200 and 400 MHz the previously reported dinuclear m-X[Gd(DTTA)$(H_2O)_2]_2^{2-}$ and p-X[Gd(DTTA)$(H_2O)_2]_2^{2-}$ complexes have relaxivities very similar to those measured for $[Gd_3L(H_2O)_6]^{3-}$ (Table 3). A direct comparison of these three systems shows practically no difference above 10 MHz in terms of molar relaxivity per Gd^{3+}. Nevertheless, one advantage of the trinuclear complex can be a more important concentration of the relaxation effect into a restricted molecular space. We have recently introduced the concept of "density of relaxivity",[8] which we defined as the paramagnetic relaxation rate enhancement per unit mass of the agent (s^{-1} g^{-1} L). The three Gd^{3+} centers present in $[Gd_3L(H_2O)_6]^{3-}$ each have a high molar relaxivity. Given the low molecular mass of the complex, this important relaxation effect is concentrated into a small molecular volume. Table 2 lists densities of relaxivity at 20 MHz for a series of Gd^{3+} complexes. For $[Gd_3L(H_2O)_6]^{3-}$ a value of 29.0 s^{-1} g^{-1} L is calculated, which is ~4 times as higher than that for the commercial $[Gd(DTPA)(H_2O)]^{2-}$ and $[Gd(DOTA)(H_2O)]^{-}$, and ~2 times more important than those for the macromolecular contrast agent Gadomer 17.

Experimental

Synthesis

All reagents were purchased from commercial sources and used without further purification. Compounds **2**, **3** and **4** were synthesized as described in ref. 25.

Synthesis of compound 5. To a stirred solution of 1,3,5-tris(bromomethyl)-2,4,6-trimethylbenzene (200 mg, 0.5 mmol) in 60 ml of dry acetonitrile was added compound **4** (1.03 g, 1.84 mmol) and K_2CO_3 (276 mg, 2.0 mmol). The resulting mixture was refluxed for 7 h (disappearance of starting material was monitored by ESI-MS). The solvent was removed *in vacuo* and the residue was redissolved in dichloromethane. This organic phase was washed three times with water, once with brine, then dried over Na_2SO_4. The solvent was removed to afford 1.11 g of a product which was used without further purification. ^{1}H NMR ($CDCl_3$ = 7.25 ppm, 400 MHz) δ: 1.42 (s, 108H), 2.35 (s, 9H), 2.56 (*t*, J = 7.2 Hz, 12H), 2.78 (*t*, J = 7.2 Hz, 12H), 3.34 (s, 24H), 3.59 (s, 6H); MS (ESI): m/z (%): 918 (100) [MH_2^{2+}]; 612.85 (50) [MH_3^{3+}].

Synthesis of compound 6. A solution of compound **5** (900 mg, 0.5 mmol) in 70 ml of HCl (6 M) was refluxed for 10 h. After evaporation to dryness, the compound was dissolved in 70 ml of water and evaporated (this procedure was repeated 3 times). The resulting solid was then dissolved in a minimum amount of H_2O, loaded onto a conditioned cation-exchange column (Bio-Rad AG 50W-X2, H^+ form, 3.0 × 9.5 cm). The column was washed with H_2O till the pH of the eluate was neutral. The absence of Cl^- was evaluated by a typical $AgNO_3/HNO_3$ test. The column was eluted with a gradient of HCl (from 0.2 to 5 M), rinsed with H_2O until neutral pH and finally eluted with a 1 M NH_3 solution. The product was concentrated from the appropriate fractions, redissolved in a minimum amount of H_2O and loaded a second time onto a cation-exchange column (Bio-Rad AG 50W-X2, H^+ form, 2.0 × 8.5 cm). The elution scheme used was the same as for the first cation-exchange resin. This time, the product was collected from the fractions 3–4 M of HCl and evaporated to dryness. Further purification was done by HPLC (Waters Corp., Milford, MA, USA). All details are given in the ESI.† Solvent evaporation of the appropriate fractions yielded the desired product (0.05 g) as a white solid. ^{1}H NMR ($D_2O \approx$ 4.80 ppm, pD = 2.0, 400 MHz) δ: 2.45 (s, 9H), 3.16 (m, 12H), 3.52 (m, 12H), 3.72 (s, 24H), 4.1 (s, 6H); MS (ESI): m/z (%): 1162.4 (30) [MH^+]; 581.8 (100) [MH_2^{2+}].

Sample preparation

$[Gd_3L(H_2O)_6]^{3-}$ was prepared by mixing the solid ligand with a $GdCl_3$ stock solution (solution prepared from Gd_2O_3 of 99.9% purity from Fluka by dissolution in excess HCl, which was evaporated off). The concentration of the metal ion was determined by complexometric titration with standardized Na_2H_2EDTA solution. A slight excess of ligand (2%) was used to ensure complete coordination of Gd^{3+}, and the pH, measured with a combined glass electrode calibrated with Metrohm buffers, was adjusted to

6.0 with addition of known amounts of NaOH (0.8 M) and HCl (0.1 M). The absence of free Gd^{3+} was controlled with the xylenol orange test.

^{17}O NMR spectroscopy

Variable-temperature ^{17}O NMR measurements were performed on Bruker DPX-400 (9.4 T, 54.2 MHz) and Bruker Avance-200 (4.7 T, 27.1 MHz) spectrometers and a Bruker VT-3000 temperature control unit was used to stabilize the temperature, which was measured by a substitution technique.[26] Transverse and longitudinal ^{17}O relaxation rates and chemical shifts were measured between 277.1 and 371.1 K. The samples were sealed in glass spheres adapted to 10 mm NMR tubes, to avoid susceptibility corrections to the chemical shifts. ^{17}O-enriched water (Irakli Gverdtsiteli Research and Technology Center on High Technologies of Isotopes and Super Pure Materials. ^{17}O: 10.5%) was added to the gadolinium-containing samples to improve the sensitivity. Longitudinal relaxation rates $1/T_1$ were obtained by the inversion recovery method and transverse relaxation rates $1/T_2$ by the Carr–Purcell–Meiboom–Gill spin-echo technique. Acidified water ($HClO_4$, pH = 3.71) was used as the external reference. The Gd^{3+} concentration of the sample was 0.0305 mol kg^{-1}.

^{1}H NMRD

The $1/T_1$ NMRD profiles were obtained at 278.0, 298.0 and 310.0 K, on a Stelar Spinmaster Fast Field-Cycling relaxometer (covering a continuous magnetic field from $B = 2.35 \times 10^{-4}$–0.47 T, proton Larmor frequencies of 0.01–20 MHz) equipped with a VTC90 temperature control unit (temperature was fixed by a gas flow and monitored by a substitution technique), on Bruker Minispecs (30, 40 and 60 MHz); and on Bruker spectrometers (50, 100, 200 and 400 MHz). The Gd^{3+} concentration of the sample was 2.00 mM.

Data analysis: ^{17}O NMR and ^{1}H NMRD

The simultaneous least-squares fit of the ^{17}O NMR and ^{1}H NMRD data were performed by the programs Visualiseur/Optimiseur on a Matlab platform, version 6.5.[27]

Molecular modeling

To assess the volume of $[Gd_3L(H_2O)_6]^{3-}$ and the distance between the Gd^{3+} ions, a molecular model was built using the CAChe program.[28] The structure of a Sr^{2+}, instead of the Gd^{3+} complex was partially optimized using molecular mechanics (MM2 force field) and semi-empirical quantum calculations (PM5 method).

Conclusions

With the objective of maximizing proton relaxivity at high magnetic field, we have synthesized a trinuclear Gd^{3+} complex based on a trimethylbenzene core bearing three diethylenetriaminetetraacetate units for lanthanide complexation. The water exchange rate of $[Gd_3L(H_2O)_6]^{3-}$, $k_{ex}^{298} = 9.0 \pm 3.0\ s^{-1}$, is twice as high as that of $[Gd(DTPA)(H_2O)]^{2-}$ which can be rationalized in terms of a more flexible inner coordination sphere, related to the bishydration of the complex. Despite the relatively small molecular weight, the complex is not fully rigid and the rotational dynamics could only be described by separating global and local motions. The flexibility is related to the CH_2 linker between the benzene core and the chelating units, which is, however, a necessary compromise in the aim of maintaining thermodynamic stability of the complex. The two inner sphere water molecules, their fast exchange, and the relatively limited flexibility of the molecule are all important factors that contribute to the remarkable proton relaxivities, particularly at high magnetic fields (r_1 = 21.6, 17.0 and 10.7 $mM^{-1}\ s^{-1}$ at 60, 200 and 400 MHz respectively, 25 °C).

Acknowledgements

We acknowledge financial support of the Swiss National Science Foundation, the Swiss State Secretariat for Education and Research (SER) and the Centre National pour la Recherche Scientifique (CNRS, France). This work was performed in the frame of the EU COST Action D38 "Metal Based Systems for Molecular Imaging Applications".

Notes and references

1 R. G. Pautler, *Physiology*, 2004, **19**, 168.
2 P. Caravan, J. J. Ellison, T. J. McMurry and R. B. Lauffer, *Chem. Rev.*, 1999, **99**, 2293.
3 *The Chemistry of Contrast Agents in Medical Magnetic Resonance Imaging*, ed. A. E. Merbach and É. Tóth, John Wiley & Sons, Chichester, 2001.
4 P. Caravan, *Chem. Soc. Rev.*, 2006, **35**, 512.
5 E. Balogh, M. Mato-Iglesias, C. Platas-Iglesias, É. Tóth, K. Djanashvili, J. A. Peters, A. de Blas and T. Rodríguez-Blas, *Inorg. Chem.*, 2006, **45**, 8719.
6 V. C. Pierre, M. Botta and K. N. Raymond, *J. Am. Chem. Soc.*, 2005, **127**, 504.
7 J. B. Livramento, É. Tóth, A. Sour, A. Borel, A. E. Merbach and R. Ruloff, *Angew. Chem., Int. Ed.*, 2005, **44**, 1504.
8 J. B. Livramento, A. Sour, A. Borel, A. E. Merbach and É. Tóth, *Chem.–Eur. J.*, 2006, **12**, 989.
9 J. B. Livramento, C. Weidensteiner, M. I. M. Prata, P. R. Allegrini, C. F. G. C. Geraldes, L. Helm, R. Kneuer, A. E. Merbach, A. C. Santos, P. Schmidt and É. Tóth, *Contrast Media Mol. Imaging*, 2006, **1**, 30.
10 J. Costa, É. Tóth, L. Helm and André E. Merbach, *Inorg. Chem.*, 2005, **44**, 4747.
11 S. Aime, M. Botta, J. I. Bruce, V. Mainero, D. Parker and E. Terreno, *Chem. Commun.*, 2001, 115.
12 In the *in vivo* imaging experiments performed with the metallostar and with the trinuclear complex $[Gd_3L(H_2O)_6]^{3-}$, the contrast agent was well tolerated by the mice. No gross side effects were observed during injection, immediately or days after the experiment.
13 P. Loureiro de Sousa, J. B. Livramento, L. Helm, A. E. Merbach, W. Même, B.-T. Doan, J.-C. Beloeil, M. I. M. Prata, A. C. Santos, C. F. G. C. Geraldes and É. Tóth, to be submitted.
14 G. M. Nicolle, L. Helm and A. E. Merbach, *Magn. Reson. Chem.*, 2003, **41**, 794.
15 D. H. Powell, O. M. Ni Dhubhghaill, D. Pubanz, L. Helm, Y. S. Lebedev, W. Schlaepfer and A. E. Merbach, *J. Am. Chem. Soc.*, 1996, **118**, 9333.
16 É. Tóth, L. Helm and A. E. Merbach, Relaxivity of Gadolinium(III) Complexes: Theory and Mechanism, in *The Chemistry of Contrast Agents in Medical Magnetic Resonance Imaging*, ed. É. Tóth and A. E. Merbach, Wiley, Chichester, 2001, p. 45.
17 (*a*) G. Lipari and S. Szabo, *J. Am. Chem. Soc.*, 1992, **10**, 4546; (*b*) G. Lipari and S. Szabo, *J. Am. Chem. Soc.*, 1992, **10**, 4559.
18 É. Tóth, L. Helm, K. E. Kellar and A. E. Merbach, *Chem.–Eur. J.*, 1999, **5**, 1202.
19 (*a*) M.-R. Spirlet, J. Rebizant, J. F. Desreux and M.-F. Loncin, *Inorg. Chem.*, 1984, **23**, 359; (*b*) J. J. Stezowski and J. L. Hoard, *Isr. J. Chem.*, 1984, **24**, 323.

20 A. M. Raitsimring, A. V. Astashkin, D. Baute, D. Goldfarb and P. Caravan, *J. Phys. Chem. A*, 2004, **108**, 7318.
21 F. A. Dunand, A. Borel and A. E. Merbach, *J. Am. Chem. Soc.*, 2002, **124**, 710.
22 R. Ruloff, T. Gelbrich, J. Sieler, E. Hoyer and L. Beyer, *Z. Naturforsch., B: Chem. Sci.*, 1997, **52**, 805.
23 G. M. Nicolle, É. Tóth, H. Schmitt-Willich, B. Radüchel and A. E. Merbach, *Chem.–Eur. J.*, 2002, **8**, 1040.
24 J. Costa, R. Ruloff, L. Burai, L. Helm and A. E. Merbach, *J. Am. Chem. Soc.*, 2005, **127**, 5147.
25 J. Platzek, U. Niedballa, B. Radüchel, DE 19508058, 1996, p. 13.
26 C. Amman, P. Meyer and A. E. Merbach, *J. Magn. Reson.*, 1982, **46**, 319.
27 (*a*) F. Yerly, *VISUALISEUR 2.3.5*, Lausanne, Switzerland, 1999; (*b*) F. Yerly, *OPTIMISEUR 2.3.5*, Lausanne, Switzerland, 1999.
28 *CACheWorksystem Pro 6.1*, Fujitsu, 2000–2003.

